

Post-selection-loophole-free Bell violation with genuine time-bin entanglement

Francesco Vedovato,^{1,2} Costantino Agnesi,¹ Marco Tomasin,¹ Marco Avesani,¹ Jan-Åke Larsson,³ Giuseppe Vallone,^{1,4} and Paolo Villoresi^{1,4}

¹Dipartimento di Ingegneria dell'Informazione, Università di Padova, via Gradenigo 6B, 35131 Padova, Italy

²Centro di Ateneo di Studi e Attività Spaziali “G. Colombo”,
Università di Padova, via Venezia 15, 35131 Padova, Italy

³Institutionen för systemteknik, Linköpings Universitet, 581 83 Linköping, Sweden

⁴Istituto di Fotonica e Nanotecnologie, CNR, via Trasea 7, 35131 Padova, Italy

(Dated: December 3, 2024)

Entanglement is an invaluable resource for fundamental tests of physics and the implementation of quantum information protocols such as device-independent secure communications. In particular, time-bin entanglement is widely exploited to reach these purposes both in free-space and optical fiber propagation, due to the robustness and simplicity of its implementation. However, all existing realizations of time-bin entanglement suffer from an intrinsic post-selection loophole, which undermines their usefulness. Here, we report the first experimental violation of Bell's inequality with “genuine” time-bin entanglement, free of the post-selection loophole. We modify the setup by replacing the first passive beam-splitter in each measurement station with an additional interferometer acting as a fast optical switch synchronized with the source. Using this setup we obtain a post-selection-loophole-free Bell violation of more than nine standard deviations. Since our scheme is fully implementable using standard fiber-based components and is compatible with modern integrated photonics, our results pave the way for the distribution of genuine time-bin entanglement over long distances.

Introduction.— In 1989 Franson conceived a simple interferometric setup to highlight the counter-intuitive implications of quantum mechanics [1]. He proposed to send a pair of entangled photons to two equal measurement stations (Alice and Bob), each composed of an unbalanced interferometer. By exploiting the quantum interference expected in the detection events recorded at the output ports of the interferometers, it should be possible to rule out local realistic models [2] by violating a Bell-CHSH inequality [3]. Franson's idea was first implemented by exploiting *energy-time* entanglement, which can be easily created by pumping a non-linear crystal with a continuous-wave (CW) laser [4–6]. In fact, the two emitted photons are generated at the same instant, but the emission time is uncertain within the coherence time of the source, thus leading to indistinguishability in the alternative paths the photons will take in the measurement stations. Extending Franson's idea, *time-bin* (TB) entanglement was introduced by Brendel *et al.* in 1999 [7]: the CW laser is replaced by a pulsed laser which shines the non-linear crystal after passing through an unbalanced “pump” interferometer. Now, the pair of photons can be emitted at two possible times, depending on the path taken by the pump-pulse in the first interferometer (see Fig. 1A). Both energy-time and time-bin entanglement have been widely used to distribute entanglement over long distances [8–12], and to realize fiber-based cryptographic systems [13, 14], aiming for device-independent security [15–17], which requires the loophole-free violation of a Bell inequality, as reported in [18–21].

However, Aerts *et al.* noted that Franson's Bell-test is intrinsically affected by the so-called *post-selection loophole* (PSL) [22], which is present independently to the other common loopholes (eg., locality and detection) that could affect local-realistic tests [23]. In fact, in Franson's configuration, Alice and Bob should post-select only the indistin-

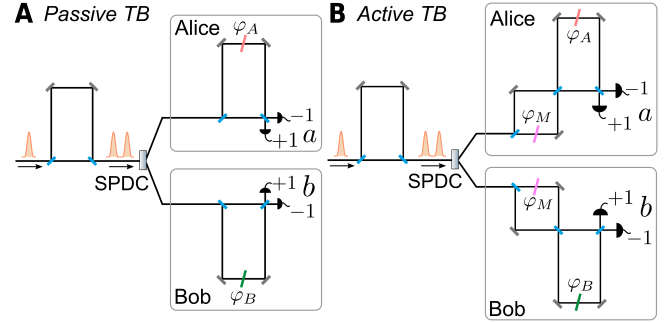


FIG. 1. *Time-bin schemes to realize a Bell-test à la Franson.* (A) In the passive TB, by post-selecting the events detected in coincidence only in the central time-slot, Alice and Bob can violate the Bell's inequality, but the scheme is affected by an intrinsic PSL. (B) In the active TB, the passive beam splitter is replaced by a balanced MZI acting as an optical switch. By exploiting a fast phase modulator φ_M in one arm of the balanced MZI, Alice and Bob can violate the Bell-CHSH inequality without discarding any data, i.e. this scheme is free of the PSL.

guishable events occurring within a coincidence window $\Delta\tau_c$, discarding those photons arriving at different times. When performing such post-selection, there exists a local-hidden-variable (LHV) model which reproduces the quantum predictions [22, 24]. The reason for this is that a LHV model admits the local delays to depend on the local parameter (φ_A or φ_B), but Alice and Bob need to compare these delays to perform the post-selection. Therefore, even though the physical system is completely local, the measurement-process post-selection invalidates the locality assumption required to derive the Bell's inequality. The same loophole affects the time-bin entanglement scheme shown in Fig. 1A, invalidating the Bell's inequality as test of local realism and enabling

the hacking of Franson's scheme when used for cryptographic purposes [25]. In this case, the Bell-test gives false evidence, since the apparent violation would tell users the setup is device-independently secure, while it is in fact insecure because of the PSL.

Many modifications to Franson's original scheme have been proposed to address the PSL, with both energy-time and time-bin entanglement. Regarding the former, a proposal by Cabello *et al.* modified the geometry of the interferometers by interlocking them in a *hug configuration*, and introduced a *local* post-selection, which does not require communication between Alice and Bob [26]. In this way, *genuine* energy-time entanglement can be generated, i.e. not affected by the PSL. Soon after this proposal had been conceived, table-top experiments were realized [27, 28] and a few years later the distribution of genuine energy-time entanglement through 1 km of optical fibers [29] and its implementation in an optical fiber-network was reported [30]. However, the hug configuration requires to stabilize two long interferometers whose extension is determined by the distance between Alice and Bob: the larger the separation is, the more demanding the stabilization becomes. In the case of time-bin entanglement, the original proposal mentioned the use of *active* switches [7], such as movable mirrors synchronized with the source, instead of passive beam splitters (Fig. 1A), to prevent discarding any data. This solution can also be exploited to overcome the PSL [24], but no such scheme has been realized so far.

Here we propose and implement, for the first time, a genuine time-bin entanglement scheme allowing the violation of a Bell's inequality free of the PSL. In our scheme, the active switches are realized by replacing the first beam splitter, in each unbalanced interferometer of the measurement stations, with another balanced interferometer with a fast phase-shifter in one arm, as sketched in Fig. 1B. By actively synchronizing the phase-shifter with the pump pulses, it is possible to use the full detection statistics, overcoming the PSL. The independence between Alice's and Bob's terminals, the relaxed stabilization requirements, as well as the compliance with off-the-shelves components open the possibility to exploit such scheme over long distances, paving the way to a conclusive loophole-free Bell-test [18–21] with time-bin entanglement.

In the following, we will analyze the time-bin passive and active schemes by making use of the POVM formalism [31], after which we will present the experiment and the obtained Bell-CHSH inequality violation attesting the faithfulness of our scheme.

Conceptual analysis of time-bin entanglement schemes.— In the passive time-bin scheme, a pump Mach-Zehnder interferometer (MZI) with a temporal imbalance equal to Δt is used to split a short light pulse into two, as sketched in Fig. 1A. This light is focused into a non-linear crystal producing photon pairs via a spontaneous parametric down conversion (SPDC) process. By optimizing the pump energy, the generation of double photon-pairs is suppressed, and the Bell state $|\Phi^+\rangle = (|S\rangle_A |S\rangle_B + |L\rangle_A |L\rangle_B) / \sqrt{2}$ is produced, where the indexes A and B represent the generated photons

that are sent to Alice's and Bob's measurement stations. Each of these is composed by an unbalanced MZI that has the same imbalance Δt of the pump-interferometer and can introduce a further phase shift φ_A (φ_B). The output ports of each interferometer are followed by two single-photon detectors, and the possible outcomes are labeled $a = \pm 1$ and $b = \pm 1$ for Alice and Bob respectively, depending on which detector clicks.

In the passive TB scheme, each photon of the pair can be detected only at three possible distinct times ($t_0 - \Delta t, t_0, t_0 + \Delta t$), due to the pump- and measurement-MZIs. By post-selecting the detection events that occur in the central time-slot only, Alice's measurement station realizes the projection $\{\hat{P}_a\}_{a=\pm 1}$ defined by $\hat{P}_a = |\psi_a\rangle\langle\psi_a|$ where $|\psi_a\rangle = (|S\rangle + a e^{i\varphi_A} |L\rangle) / \sqrt{2}$, and similar relations hold for Bob's measurement station (with a replaced by b and A by B). Since the delay is local, one could think that this should allow the violation of the Bell's inequality. There is simply no physical mechanism for the remote phase shift to influence the local delay. However, for a coincidence to occur, Bob's delay needs to coincide with Alice's, and Bob's delay is controlled by Bob's phase shift, remotely from the point of view of Alice. This constitutes a coincidence loophole for the Bell inequality [32], somewhat similar to a detection loophole with 50% detection efficiency, but much worse since it is present even when using loss-free equipment, therefore introducing an unavoidable intrinsic loophole in the setup.

Quantum mechanics provides the probabilities $\mathcal{P}_{a,b}$ for photon detections that occur within a coincidence window $\Delta\tau_c < \Delta t$ around the central time-slot for each pair of detectors a, b . The probabilities $\mathcal{P}_{a,b}$ depend on the initial state $|\Phi^+\rangle$ and on the local phase shifts φ_A, φ_B introduced by the measurement stations and are given by $\mathcal{P}_{a,b}(\varphi_A, \varphi_B) = \frac{1}{4} [1 + ab\mathcal{V} \cos(\varphi_A + \varphi_B)]$, where \mathcal{V} is the visibility of two-photon interference.

Disregarding the PSL, the interference in the post-selected events will seem to violate the Bell-CHSH inequality, which provides an upper limit for a combination of four correlation functions $E(\varphi_A, \varphi_B)$ with different phases φ_A, φ_B , when assuming the existence of a LHV model [3]. The correlation function is given by $E(\varphi_A, \varphi_B) = \sum_{a,b} ab\mathcal{P}_{a,b}(\varphi_A, \varphi_B)$ and the Bell-CHSH inequality $S \leq 2$ [3] is given in terms of the S -parameter $S \equiv E(\varphi_A, \varphi_B) + E(\varphi'_A, \varphi_B) + E(\varphi_A, \varphi'_B) - E(\varphi'_A, \varphi'_B)$, where φ_A, φ'_A and φ_B, φ'_B denote the values of the phase-shifts introduced by Alice and Bob respectively. Quantum mechanics predicts the correlation function $E^{\text{QM}}(\varphi_A, \varphi_B) = \mathcal{V} \cos(\varphi_A + \varphi_B)$, which leads to a maximum value for the S -parameter equal to $S_{\text{max}} = 2\sqrt{2}\mathcal{V}$ for the settings $\varphi_A = -\pi/4, \varphi'_A = \pi/4$ and $\varphi_B = 0, \varphi'_B = \pi/2$. Hence, the Bell-CHSH inequality will seem to be violated only if $\mathcal{V} > 1/\sqrt{2} \approx 0.71$.

It is worth noticing that if no post-selection is applied in the passive TB scheme, then the Bell-CHSH inequality does hold, and could in principle be violated. However, in this case Alice's measurement station implements the POVM given by $\{\hat{\Gamma}_a\}_{a=\pm 1}$ with $\hat{\Gamma}_a = (1/4)\mathbb{1} + (1/2)\hat{P}_a$, where $\mathbb{1} = |S\rangle\langle S| + |L\rangle\langle L|$ (and similar relations hold for Bob). Thus, with no

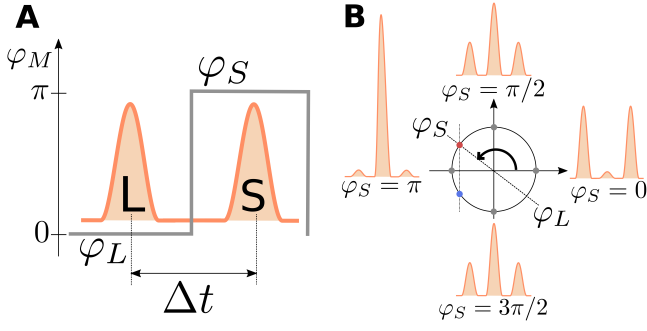


FIG. 2. *Functioning of the active TB scheme.* (A) In a balanced MZI, the relative phase φ_M sensed by a traveling pulse determines the output port it will exit at with probabilities $\cos^2(\varphi_M/2)$ and $\sin^2(\varphi_M/2)$. By using a fast modulator, it is possible to impose the different phase-shifts φ_S and φ_L to the $|S\rangle$ and $|L\rangle$ photons while they are traveling along the balanced MZI. By fixing $\varphi_S = \pi$ and $\varphi_L = 0$, it is possible to temporally recombine $|S\rangle$ and $|L\rangle$ pulses, making them indistinguishable. (B) The detection pattern at the output ports depends on the values φ_S and $\varphi_L = \varphi_S - \pi$. If $\varphi_S = \pi$, all detection events occur in the central time-slot, whereas if $\varphi_S = 0$ they are present only in the lateral time-slots. Any other detection histogram can be obtained with two different φ_S values, one with $\varphi_S < \pi$ (red dot) and the other with $\varphi_S > \pi$ (blue dot). For example, $\varphi_S = \pi/2$ and $\varphi_S = 3\pi/2$ have the same click distribution.

post-selection, the quantum probabilities $\mathcal{P}_{a,b}$ for photon detections at the two stations lead to a maximum value for the S-parameter that can be written as $S_{\max} = 2\sqrt{2}\mathcal{V}'$, with the overall three-peak visibility $\mathcal{V}' = \mathcal{V}/4$ and the Bell-CHSH inequality can not be violated even with perfect visibility $\mathcal{V} = 1$.

On the other hand, a proper violation can be achieved in the active TB scheme here proposed (see Fig. 1B). We replace the passive beam-splitter with an additional balanced MZI acting as a fast optical switch, which allows the measurement MZI to recombine the $|S\rangle$ and $|L\rangle$ pulses, making them indistinguishable. In this way, contrary to the passive TB scheme which recombines the two temporal modes in a probabilistic manner, our scheme deterministically compensates for the delay Δt and no detections are discarded. Indeed, by imposing the phases φ_S and $\varphi_L = \varphi_S - \pi$ on the $|S\rangle$ and $|L\rangle$ pulses respectively, the balanced MZI determines the path they will take in the measurement MZI, as sketched in Fig. 2A.

At each detector, we expect a detection pattern that depends on the value of φ_S , as shown in Fig. 2B. From a formal point of view, in our TB scheme Alice's measurement station implements the POVM $\{\hat{\Pi}_a\}_{a=\pm 1}$, where $\hat{\Pi}_a = \frac{1}{2} (\cos^2 \frac{\varphi_S}{2} |S\rangle\langle S| + \sin^2 \frac{\varphi_S}{2} |L\rangle\langle L|) + |\chi_a\rangle\langle\chi_a|$ with $|\chi_a\rangle = (ie^{-i\frac{\varphi_S}{2}} \sin \frac{\varphi_S}{2} |S\rangle + ae^{i(\varphi_A - \frac{\varphi_L}{2})} \cos \frac{\varphi_L}{2} |L\rangle)/\sqrt{2}$ (the phase difference between the transmitted and reflected mode by a beam splitter is $e^{i\pi/2} = i$). If $\varphi_L = \varphi_S - \pi$, the POVM reduces to

$$\hat{\Pi}_a = \frac{1}{2} \cos^2 \left(\frac{\varphi_S}{2} \right) \mathbb{1} + \sin^2 \left(\frac{\varphi_S}{2} \right) \hat{P}_a. \quad (1)$$

If Alice sets the phase $\varphi_S = \pi$ (and thus $\varphi_L = 0$), $\hat{\Pi}_a$ reduces to \hat{P}_a and her station actually projects onto the state $|\psi_a\rangle$, with no post-selection procedure. Indeed, in the detection pattern the lateral peaks “disappear”, as shown in Fig. 2B and it is not necessary to discard any data. Hence, the violation of Bell-CHSH inequality expected from our scheme is free of the PSL.

Description of the experiment.— We implemented the active TB scheme proposed above by using the experimental setup sketched in Fig. 3. A mode-locking laser produced a pulse train with wavelength centered around 808 nm, 76 MHz of repetition rate and ~ 150 fs of pulse duration. This beam is used to pump a second-harmonic-generation (SHG) crystal which generates coherent pulses of light up-converted to 404 nm. Each of the obtained pulse passes through a free-space unbalanced Michelson interferometer (that is the pump-interferometer) which produces a coherent state in two temporal modes. The imbalance $\Delta l = L - S$ between the two arms is about 90 cm, corresponding to a temporal imbalance $\Delta t = \Delta l/c \approx 3$ ns (with c the speed of light in vacuum), much greater than the coherence time of the pulses. Then, the pulses pump a 2-mm long Beta-Barium Borate (BBO) crystal to produce the entangled photon state via type II SPDC [33] at 808 nm.

The two photons are sent to Alice' and Bob's terminals after being spectrally filtered (3 nm bandwidth) and collected by two single-mode optical fibers. Each station is composed of two MZIs, a balanced one and an unbalanced one. The balanced MZI is composed by a 50:50 fiber coupler which defines the two arms of the interferometer. To guarantee the zero imbalance of this MZI, a nanometric slit is placed in one of the two arms.

The balanced MZI works as a fast optical switch, since there is a fast (\sim GHz bandwidth) phase-modulator in one of its arms. The modulation voltage is set to V_π such that $\varphi_S - \varphi_L = \pi$, while the DC bias of the phase-modulator is driven by an external proportional-integral-derivative (PID)

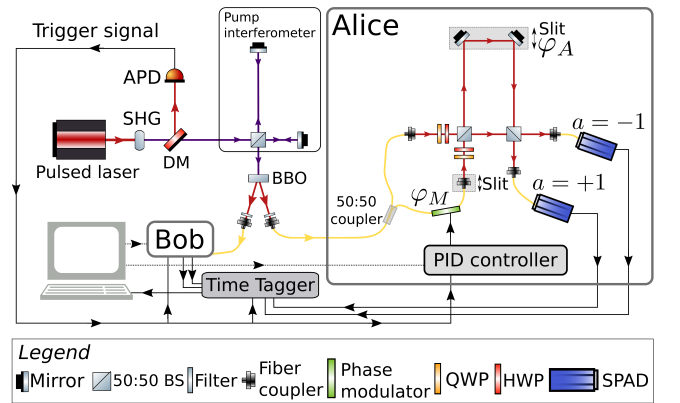


FIG. 3. *Experimental setup to implement the active TB scheme.* Bob's measurement station is analogue to Alice's one. APD: analog-photo-detector; DM: dichroic mirror.

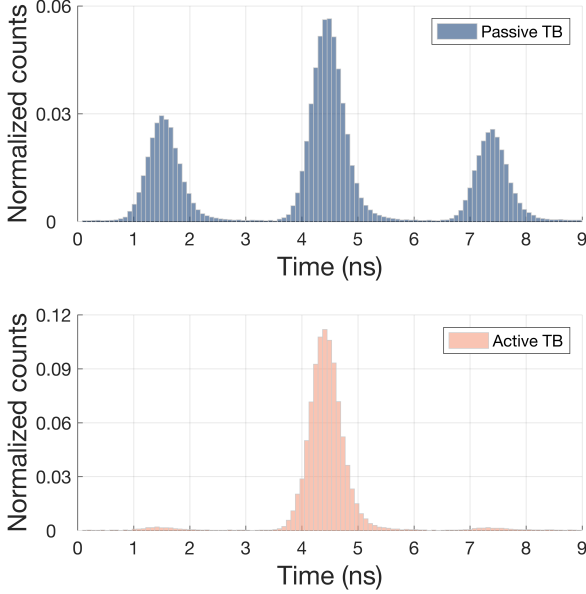


FIG. 4. *Typical detection histograms obtained during data acquisition.* The two histograms represent all the raw detections collected by one of the four detectors during the data acquisition. The blue histogram shows a typical detection pattern obtained with the passive TB scheme, in which the three-peak profile is observed. The orange histogram shows the detection pattern obtained with the active TB scheme: the PID controller is able to lock φ_S to π and φ_L to 0, thus making the lateral peak disappear, allowing us to realize a time-bin Bell-test free of the PSL. The counts are normalized to fairly compare the two histograms.

controller, that is responsible of locking the phase φ_S to π . The complete operating principle of the PID controller is detailed in the Supplementary Material.

The two arms of the balanced MZI are recombined at a 50:50 free-space beam splitter (BS) after been optimized for polarization rotations. This BS begins the unbalanced MZI whose imbalance is equal to that of the pump-interferometer (within the coherence time $\sim 200 \mu\text{s}$ of the photons). The two mirrors of the long arm of the unbalanced MZI are placed on a nanometric piezoelectric slit to both guarantee the required imbalance Δt and introduce the local phase shift φ_A and φ_B to realize the Bell-test. At the two output ports of the measurement stations we used two avalanche single photon detectors (SPADs, $\sim 50\%$ detection efficiency), labeled as $a = \pm 1$ and $b = \pm 1$. The detection events are then time-tagged by a time-to-digital converter (Time Tagger) with 81 ps resolution and the data are stored in a PC.

Results of the Bell-test.— With the setup shown in Fig. 3, we performed the time-bin Bell-test with three different schemes: I) the *passive TB with post-selection*, II) the *passive TB with no post-selection* III) the *active TB with no post-selection* proposed above. To realize I), we bypassed the balanced MZI in each of the measurement stations, hence obtaining the passive TB configuration of Fig. 1A. By choosing

a coincidence window $\Delta\tau_c \approx 2.4 \text{ ns}$ and by post-selecting the coincident events that occurred only in the central time-slot, Alice (Bob) implemented the projective measurement given by \hat{P}_a (\hat{P}_b) and the expected Bell-CHSH violation is affected by the PSL. To realize II), we used the same configuration as in I), but we did not discard any data by choosing a coincidence window $\Delta\tau_c \approx 8.1 \text{ ns}$, which corresponds to the total width of the three peak-profile in the detections (see Fig. 4). In this case, Alice (Bob) implemented the POVM given by $\hat{\Gamma}_a$ ($\hat{\Gamma}_b$) and no Bell-CHSH violation is expected.

To implement III), we exploited the balanced MZI in each station and we used the PID controller to lock the phase φ_S and φ_L to π and 0 respectively, independently at each terminal. We did not discard any data by choosing a large coincidence window as in II), but, in this case, the Bell-CHSH inequality is directly applicable, since Alice (and Bob) implemented the POVM given in (1) with $\varphi_S = \pi$. The expected Bell-CHSH violation is free of the post-selection loophole and this represents the main result of our work.

We show in Fig. 4 a typical detection histogram obtained with one of the four detectors during the data acquisition (the results are similar for all the detectors). In the case of TB schemes I) and II), since the balanced MZI is bypassed, we obtained the expected three-peak profile (blue histogram). On the other hand, in our active TB scheme III), the PID controller makes the lateral peaks disappear, as shown by the orange detections histogram. This guarantees the correct functioning of the PID controller, whose details are described in the Supplementary Material. It is worth noticing that the whole three-peak profile is within the chosen coincidence window $\Delta\tau_c = 8.1 \text{ ns}$, thus guaranteeing that no data is discarded.

To realize each of the Bell-tests described above, we first calibrated the shifts to be introduced by the nanometric slits in Alice' and Bob's unbalanced MZIs. This is obtained by scanning the coincidence rate for a pair of detector by moving Bob' slit while Alice's one is fixed. From the sinusoidal pattern obtained in such a way, we estimated the experimental visibility \mathcal{V}_{exp} for each scheme. Then, we imposed the shifts (φ_A, φ_B) needed to obtain the maximal violation of the Bell inequality (as described above) and acquired the data for sufficient time to achieve significant statistics.

The results obtained for each of the three schemes described above are represented in Table I. As expected, violation of the Bell-CHSH inequality was obtained with the first and the third scheme with clear statistical evidence, but only the third one is

Scheme	$\Delta\tau_c$	PSL	\mathcal{V}_{exp}	S_{exp}	SD
I) passive TB	2.4 ns	Yes	0.95 ± 0.05	2.58 ± 0.03	18.3
II) passive TB	8.1 ns	No	0.23 ± 0.02	0.67 ± 0.02	—
III) active TB	8.1 ns	No	0.89 ± 0.03	2.30 ± 0.03	9.3

TABLE I. *Main results.* SD refers to Standard Deviation of the Bell-CHSH violation.

not affected by the PSL. The minor violation obtained in III) is due to imperfection in the balanced MZI alignment and in the locking procedure occurring during data acquisitions needed to experimentally estimate the S-parameter S_{exp} . It is worth stressing that any imperfection in the locking mechanism setting $\varphi_S = \pi$ corresponds to an effective lower visibility, but it does not introduce any loophole in the Bell inequality.

Conclusions.— Time-bin encoding [7] is a valid resource for both performing fundamental tests of quantum mechanics [34–36] and distributing entanglement over long distances [12]. However, all the time-bin entanglement realizations performed so far were affected by the post-selection loophole, which makes this technique unsuitable for quantum information protocols. A possible way to overcome this problem requires to violate the so-called “chained” Bell-inequalities [37], but the needed visibility ($\gtrsim 0.94$ [25]) is considerably higher than the one of the Bell-CHSH inequality ($\gtrsim 0.71$). Even if such a high visibility is achievable with time-bin entanglement, as shown in [38], our scheme clearly relaxes this requirement, since the Bell-CHSH inequality is directly applicable.

This work is the first implementation of genuine time-bin entanglement, and represents a crucial step towards its exploitation for fundamental tests of physics and the realization of the quantum internet [39]. In fact, our scheme can be realized using only commercial off-the-shelves fiber components and, since its stability does not depend on the distance between Alice and Bob, it is easier to be implemented with respect to the hug configuration [26]. Furthermore, as long as both the π -phase transition imposed by the modulator and the detectors jitter are shorter than the imbalance Δt , it is possible to shorten it, rendering it compatible with today’s photonic integrated technologies [40, 41]. Finally, our work makes time-bin entanglement a viable technique to obtain a loophole-free Bell violation, that is the enabling ingredient of any device-independent protocol [15–17, 42].

SUPPLEMENTARY MATERIAL

Operating principle of the PID controller.— In our experiment we drive the phase φ_M introduced by the phase-modulator (PM) in the balanced MZI to make the photons take a precise path in the subsequent MZI. To realize this, we implemented the PID controller that is sketched in Fig. 5.

First, we synchronize the phase transition with the pump-pulses that produce the photon pair. This is performed by a fast analog-photo-diode (APD) that collects the 808 nm pulsed beam (after being separated with a dichroic mirror (DM) from the 404 nm pulse train produced by the SHG stage, see Fig. 3) and produces an electric signal synchronized with the optical pulses. This signal is split in two: one is then collected by the time-tagger for timing purposes and the other one is sent to the PID controller.

The first stage of the PID controller is an amplifier (iXblue)

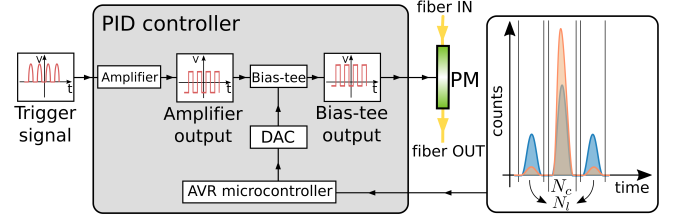


FIG. 5. Detailed scheme of the PID controller.

which produces a square wave with fixed amplitude centered around 0 V. The amplitude V_π of this wave set the strength $\Delta\varphi = \varphi_S - \varphi_L = \pi$ of the transition introduced by the phase-modulator. The raise time of the square wave is less than 2.5 ns to guarantee that the π -transition occurs within the short-long temporal separation Δt .

The absolute value of the phase φ_S of the balanced MZI is perturbed by temperature fluctuations and vibrations due to the environment. In order to correctly implement our scheme, we have to compensate this phase fluctuation (which occurs in the order of tens of seconds), by locking the value of φ_S to π .

To perform this locking, the second stage of the PID controller is given by a bias-tee (MiniCircuits) which compensates the intrinsic phase shift of the balanced MZI by changing the offset voltage V_{bias} of the square wave produced by the amplifier. This is obtained by the combined action of an AVR micro-controller (Arduino) and a digital-to-analog converter (DAC) by maximizing the extinction ratio R between the central and the lateral peaks $R = (N_c - N_l) / (N_c + N_l)$, where N_c are the counts associated to the central peak and N_l are all the counts in the lateral ones recorded by one of the two detectors of the measurement station. All the counts in each detector can be estimated in real-time by looking at the raw data collected by the time-tagger (QuTools), and they produce the detection histogram sketched in the inset of Fig. 5, which corresponds to the real detection histograms presented in Fig. 4.

To successfully lock φ_S to π the PID controller has to first evaluate its real-time value by observing the detection histogram and computing R . Unfortunately, there is no one-to-one correspondence between the extinction ratio and the phase φ_S . Indeed, for each possible value of R there exist two possible values for φ_S that reproduce the observed histograms (with the exception of 0 and π), as shown in Fig. 2B. Therefore, we must include an additional information that allows us to distinguish between the two possible phase values. This information is given by the derivative of the extinction ratio. If an increase of the phase value causes an increase of the ratio, we choose the phase $0 < \varphi_S < \pi$ (requiring further increase to reach π). Otherwise, we choose the phase $\pi < \varphi_S < 2\pi$ (requiring a decrease to reach π). Since the PID requires an error function that is equal to zero when the objective is reached, we choose the function $E_{\varphi_S} = \text{sgn} \left(\frac{dR}{d\varphi_S} \right) \frac{N_l}{N_c}$, which guaran-

tees that the PID's objective is both to lock the value of φ_S to π and to identify correctly the value of the phase, since the symmetry between the two possible phase values is broken by the sign of the derivative of the extinction ratio.

-
- [1] J. D. Franson, *Bell inequality for position and time*, *Phys. Rev. Lett.* **62**, 2205 (1989)
 - [2] J. S. Bell, *On the Einstein Podolsky Rosen paradox*, Physics (Long Island City, NY) **1**, 195 (1964)
 - [3] J. F. Clauser, M. A. Horne, A. Shimony, R. A. Holt, *Proposed Experiment to Test Local Hidden-Variable Theories*, *Phys. Rev. Lett.* **23**, 880 (1969)
 - [4] Z. Y. Ou, X. Y. Zou, L. J. Wang, L. Mandel, *Observation of nonlocal interference in separated photon channels*, *Phys. Rev. Lett.* **65**, 321 (1990)
 - [5] J. Brendel, E. Mohler, W. Martienssen, *Experimental Test of Bell's Inequality for Energy and Time*, *Europhys. Lett.* **20**, 575 (1992)
 - [6] P. G. Kwiat, A. M. Steinberg, R. Y. Chiao, *High-visibility interference in a Bell-inequality experiment for energy and time*, *Phys. Rev. A* **47**, R2472(R) (1993)
 - [7] J. Brendel, N. Gisin, W. Tittel, H. Zbinden, *Pulsed Energy-Time Entangled Twin-Photon Source for Quantum Communication*, *Phys. Rev. Lett.* **82**, 2594 (1999)
 - [8] P. R. Tapster, J. G. Rarity, P. C. M. Owens, *Violation of Bell's Inequality over 4 km of Optical Fiber*, *Phys. Rev. Lett.* **73**, 1923 (1994)
 - [9] W. Tittel, J. Brendel, H. Zbinden, N. Gisin, *Violation of Bell Inequalities by Photons More Than 10 km Apart*, *Phys. Rev. Lett.* **81**, 3563 (1998)
 - [10] W. Tittel, J. Brendel, N. Gisin, H. Zbinden, *Long-distance Bell-type tests using energy-time entangled photons*, *Phys. Rev. A* **59**, 4150 (1999)
 - [11] I. Marcikic, H. de Riedmatten, W. Tittel, H. Zbinden, M. Legré, N. Gisin, *Distribution of Time-Bin Entangled Qubits over 50 km of Optical Fiber*, *Phys. Rev. Lett.* **93**, 180502 (2004)
 - [12] T. Inagaki, N. Matsuda, O. Tadanaga, M. Asobe, H. Takesue, *Entanglement distribution over 300 km of fiber*, *Opt. Express* **21**, 23241 (2013)
 - [13] W. Tittel, J. Brendel, H. Zbinden, N. Gisin, *Quantum Cryptography Using Entangled Photons in Energy-Time Bell States*, *Phys. Rev. Lett.* **84**, 4737 (2000)
 - [14] N. Gisin, G. Ribordy, W. Tittel, H. Zbinden, *Quantum cryptography*, *Rev. Mod. Phys.* **74**, 145 (2002)
 - [15] A. Acín, N. Gisin, L. Masanes, *From Bells Theorem to Secure Quantum Key Distribution*, *Phys. Rev. Lett.* **97**, 120405 (2006)
 - [16] A. Acín, N. Brunner, N. Gisin, S. Massar, S. Pironio, V. Scarani, *Device-Independent Security of Quantum Cryptography against Collective Attacks*, *Phys. Rev. Lett.* **98**, 230501 (2007)
 - [17] R. Arnon-Friedman, F. Dupuis, O. Fawzi, R. Renner, T. Vidick, *Practical device-independent quantum cryptography via entropy accumulation*, *Nat. Commun.* **9**, 459 (2018)
 - [18] B. Hensen, H. Bernien, A. E. Dréau, A. Reiserer, N. Kalb, M. S. Blok, J. Ruitenbergh, R. F. L. Vermeulen, R. N. Schouten, C. Abellán, W. Amaya, V. Pruneri, M. W. Mitchell, M. Markham, D. J. Twitchen, D. Elkouss, S. Wehner, T. H. Taminiau, R. Hanson, *Loophole-free Bell inequality violation using electron spins separated by 1.3 kilometres*, *Nature* **526**, 682-686 (2015)
 - [19] M. Giustina, M. A. M. Versteegh, S. Wengerowsky, J. Handsteiner, A. Hochrainer, K. Phelan, F. Steinlechner, J. Kofler, J.-Å. Larsson, C. Abellán, W. Amaya, V. Pruneri, M. W. Mitchell, J. Beyer, T. Gerrits, A. E. Lita, L. K. Shalm, S. W. Nam, T. Scheidl, R. Ursin, B. Wittmann, A. Zeilinger, *Significant-Loophole-Free Test of Bells Theorem with Entangled Photons*, *Phys. Rev. Lett.* **115**, 250401 (2015)
 - [20] L. K. Shalm, E. Meyer-Scott, B. G. Christensen, P. Bierhorst, M. A. Wayne, M. J. Stevens, T. Gerrits, S. Glancy, D. R. Hamel, M. S. Allman, K. J. Coakley, S. D. Dyer, C. Hodge, A. E. Lita, V. B. Verma, C. Lambrocco, E. Tortorici, A. L. Migdall, Y. Zhang, D. R. Kumor, W. H. Farr, F. Marsili, M. D. Shaw, J. A. Stern, C. Abellán, W. Amaya, V. Pruneri, T. Jennewein, M. W. Mitchell, P. G. Kwiat, J. C. Bienfang, R. P. Mirin, E. Knill, S. W. Nam, *Strong Loophole-Free Test of Local Realism*, *Phys. Rev. Lett.* **115**, 250402 (2015)
 - [21] W. Rosenfeld, D. Burchardt, R. Garthoff, K. Redeker, N. Ortel, M. Rau, H. Weinfurter, *Event-Ready Bell Test Using Entangled Atoms Simultaneously Closing Detection and Locality Loopholes*, *Phys. Rev. Lett.* **119**, 010402 (2017)
 - [22] S. Aerts, P. Kwiat, J.-Å. Larsson, and M. Żukowski, *Two-Photon Franson-Type Experiments and Local Realism*, *Phys. Rev. Lett.* **83**, 2872 (1999)
 - [23] J.-Å. Larsson, *Loopholes in Bell inequality tests of local realism*, *J. Phys. A: Math. Theor.* **47**, 424003 (2014)
 - [24] J. Jogenfors, J.-Å. Larsson, *Energy-time entanglement, elements of reality, and local realism*, *J. Phys. A* **47**, 424032 (2014)
 - [25] J. Jogenfors, A. M. Elhassan, J. Ahrens, M. Bourennane, J.-Å. Larsson, *Hacking the Bell test using classical light in energy-time entanglement-based quantum key distribution*, *Sci. Adv.* **1**, e1500793 (2015)
 - [26] A. Cabello, A. Rossi, G. Vallone, F. De Martini, P. Mataloni, *Proposed Bell Experiment with Genuine Energy-Time Entanglement*, *Phys. Rev. Lett.* **102**, 040401 (2009)
 - [27] G. Lima, G. Vallone, A. Chiuri, A. Cabello, P. Mataloni, *Experimental Bell-inequality violation without the postselection loophole*, *Phys. Rev. A* **81**, 040101 (2010)
 - [28] G. Vallone, I. Gianani, E. B. Inostroza, C. Saavedra, G. Lima, A. Cabello, P. Mataloni, *Testing Hardy nonlocality proof with genuine energy-time entanglement*, *Phys. Rev. A* **83**, 042105 (2011)
 - [29] Á. Cuevas, G. Carvacho, G. Saavedra, J. Cariñe, W. A. T. Nogueira, M. Figueroa, A. Cabello, P. Mataloni, G. Lima, G. B. Xavier, *Long-distance distribution of genuine energy-time entanglement*, *Nat. Commun.* **4**, 2871 (2013)
 - [30] G. Carvacho, J. Cariñe, G. Saavedra, Á. Cuevas, J. Fuenzalida, F. Toledo, M. Figueroa, A. Cabello, J.-Å. Larsson, P. Mataloni, G. Lima, G. B. Xavier, *Postselection-Loophole-Free Bell Test Over an Installed Optical Fiber Network*, *Phys. Rev. Lett.* **115**, 030503 (2015)
 - [31] A. Peres, *Quantum Theory: Concepts and Methods*, Kluwer Academic Publishers (1993)
 - [32] J.-Å. Larsson, R. D. Gill, *Bells inequality and the coincidence-time loophole*, *Europhys. Lett.* **67**, 707713 (2004)
 - [33] P. G. Kwiat, K. Mattle, H. Weinfurter, A. Zeilinger, A. V. Sergienko, Y. Shih, *New High-Intensity Source of Polarization-Entangled Photon Pairs*, *Phys. Rev. Lett.* **75**, 4337 (1995)
 - [34] I. Marcikic, H. de Riedmatten, W. Tittel, H. Zbinden, N. Gisin, *Long-distance teleportation of qubits at telecommunication wavelengths*, *Nature* **421**, 509513 (2003)
 - [35] G. Vallone, D. Dequal, M. Tomasin, F. Vedovato, M. Schiavon, V. Luceri, G. Bianco, P. Villoresi, *Interference at the Single Photon Level Along Satellite-Ground Channels*, *Phys. Rev.*

- Lett. **116**, 253601 (2016)
- [36] F. Vedovato, C. Agnesi, M. Schiavon, D. Dequal, L. Calderaro, M. Tomasin, D. G. Marangon, A. Stanco, V. Luceri, G. Bianco, G. Vallone, P. Villoresi, *Extending Wheelers delayed-choice experiment to space*, [Sci. Adv. **3**, e1701180 \(2017\)](#)
- [37] S. Braunstein, C. M. Caves, *Wringing out better Bell inequalities*, [Ann. Phys. **202**, 22 \(1990\)](#)
- [38] M. Tomasin, E. Mantoan, J. Jogenfors, G. Vallone, J.-Å. Larsson, and P. Villoresi, *High-visibility time-bin entanglement for testing chained Bell inequalities*, [Phys. Rev. A **95**, 032107 \(2017\)](#)
- [39] H. J. Kimble, *The quantum internet*, [Nature **453**, 1023-1030 \(2008\)](#)
- [40] P. Sibson, J. E. Kennard, S. Stanisic, C Erven, J. L. OBrien, M G. Thompson, *Integrated silicon photonics for high-speed quantum key distribution*, [Optica **4**, 172-177 \(2017\)](#)
- [41] V. Sorianello, M. Midrio, G. Contestabile, I. Asselberghs, J. Van Campenhout, C. Huyghebaert, I. Goykhman, A. K. Ott, A. C. Ferrari, M. Romagnoli, *Graphenesilicon phase modulators with gigahertz bandwidth*, [Nat. Photonics **12**, 4044 \(2018\)](#)
- [42] A. Acín, L. Masanes, *Certified randomness in quantum physics*, [Nature **540**, 213219 \(2016\)](#)